# Self-Limiting Feedback between Baroclinic Waves and a NAO-like Sheared Zonal Flow

Masahiro Watanabe

Center for Climate System Research,

University of Tokyo, Kashiwa, Japan

January 7, 2009

Submitted to GRL

Corresponding author:
M. Watanabe,
Center for Climate System Research, University of Tokyo,
Kashiwa, Chiba 277-8568, Japan
(e-mail: hiro@ccsr.u-tokyo.ac.jp)

**Abstract.** The eddy-mean flow interaction associated with the North Atlantic Oscillation (NAO) is examined by means of the baroclinic wave life cycle experiments. When a sheared zonal flow perturbation akin to the NAO-related dipole wind anomaly is added to the basic state, momentum fluxes due to baroclinic waves tend to reinforce the initial zonal flow dipole in the upper troposphere both for the anticyclonic and cyclonic shears. The eddy feedback is stronger for the anticyclonic shear because the node of the dipole flow is asymmetric about the basic jet, suggesting that the positive NAO is more favored by the eddy feedback. For the zonal wind anomaly with extremely large amplitude, the baroclinic wave breaking cannot efficiently intensify the zonal flow dipole, indicating a self-limitation in the positive eddy feedback to the NAO-like zonal flow anomaly.

## 1. Introduction

The extratropical circulation variability is often separated into high- and low-frequency components based on their dynamical origin. The former is dominated by synoptic-scale baroclinic waves having the time scale of several days whereas the latter, containing various time scales from week to season, is dominated by several horizontal patterns. The archetypal in the Northern Hemisphere (NH) winter is the North Atlantic Oscillation (NAO), and its hemispheric extension called the northern annular mode (NAM). The NAO/NAM has the center of action over the North Atlantic, but also

accompanies significant zonal-mean flow anomalies characterized by a meridional dipole between the subtropics and high latitudes.

Among mechanisms so far proposed to explain why the NAO/NAM is dominant, the primary candidate is an interaction with the synoptic eddy activity, or the storm track [*Lau* 1988; *Kug and Jin* 2009]. Theoretical studies [e.g., *Lorenz and Hartmann* 2003; *Vallis et al.* 2004; *Jin et al.* 2006a,b] show that the synoptic eddies, which can often be assumed to be stochastic, are systematically stirred by the low-frequency flow anomaly, and positively feedback on it via the momentum flux anomalies. This interaction is approximated by linear process in the above studies, but nonlinearity will not be negligible when the anomalies have finite amplitude.

In general, momentum fluxes due to synoptic waves occur when they break, which is strongly nonlinear. Indeed, recent studies point out that the NAO accompanies systematic changes in the wave breaking process of the synoptic eddies [*Franzke et al.* 2004; *Martius et al.* 2007; *Riviere and Orlanski* 2007]. Therefore, in this paper, the eddy feedback to the NAO is examined with a fully nonlinear dynamics. To do so, we perform the so-called baroclinic wave life cycle experiments, in which the eddy-mean flow interaction is treated as initial-value problem [*Simmons and Hoskins* 1978]. Although the NAO/NAM has a regional feature associated with stationary eddies, we simplify the problem by ignoring the longitudinal dependence.

## 2. Baroclinic wave life cycle experiments

We use a nonlinear dynamical core of the atmospheric component model of the climate model MIROC [*Hasumi and Emori* 2004], which is jointly developed at the Center for Climate System Research (CCSR), the University of Tokyo, the National Institute for Environmental Studies (NIES), and the Frontier Research Center for Global Change (FRCGC). This is a global spectral model based on the dry primitive equations on a sphere, and the linear version of this dynamical model has been extensively used for the diagnostic studies of teleconnections [e.g., *Watanabe and Kimoto* 2000; *Watanabe and Jin* 2004]. The horizontal resolution is T63 and vertically 20 σ-levels are adopted. The dissipation included is only a $\nabla^6$ horizontal diffusion with the damping time scale of 2h for the smallest-scale wave.

The life cycle experiment is performed with a given initial perturbation imposed on a baroclinically unstable, zonally uniform initial state to simulate the perturbation growth and decay together with the stabilization of the initial state during 30 days. Since we focus on the boreal winter circulation over the North Atlantic, an idealized basic zonal-mean state is constructed by referring to the December-February (DJF) climatology of the NCEP/NCAR reanalysis [*Kistler et al.* 2001] averaged over the Atlantic sector of 90° W-30° E. The observed Atlantic jet is tilted to north-east; therefore the sector-averaged zonal wind has a broad meridional structure having the maximum of 41 $ms^{-1}$ at 38° N (Figure 1a). The idealized basic

state zonal wind is then defined as $\bar{U}_b = A(z)\sin^3(\pi \sin\varphi)$, where $\varphi$ is latitude, the over bar denotes zonal uniform quantity, and $A(z)$ gives the vertical structure taken from the observed zonal wind profile at 38° N (Figure 1c). The basic state meridional wind is set to zero while temperature field is calculated from $\bar{U}_b$ using the thermal wind relationship.

A series of the life cycle experiments is carried out by adding zonal flow anomalies having a meridional dipole pattern akin to the observed NAO-related zonal flow anomaly (Figure 1a). In this study, the NAO is defined by the leading EOF (38% fractional variance) to the winter geopotential height anomalies at 250 hPa over the Atlantic region of 100° W-30° E, 20° -80° N during 1948-2000. The anomalous zonal wind, denoted as $\bar{U}_a$, is also idealized (Figure 1c), and is scaled such as to have the maximum of 1 $ms^{-1}$. The initial wind is thus given by

$$\bar{U}\big|_{t=0} = \bar{U}_b + \alpha \bar{U}_a \quad ,$$

where $\alpha$ is a parameter controlling the amplitude of the NAO-like flow anomaly, varying from -15 to +15. It is noted that $\bar{U}_a$ is close to equivalent barotropic but does accompany the balanced temperature anomaly, which indicates that the low-level baroclinicity also changes depending on $\alpha$. For seeding the baroclinic waves, initial perturbation is imposed to surface pressure with the amplitude of 1 hPa [*Simmons and Hoskins* 1978]. The perturbation structure follows the most unstable normal mode obtained by using the T21 linearized model. While the eddy life cycle behavior may

depend on the zonal wavenumber, $k$ [*Orlanski* 2003; *Wittman et al.* 2007], we choose $k$=6 since the wave has the largest growth rate and typical of the growing baroclinic waves.

## 3. Results

The eddy fluxes associated with the imposed dipole flow anomaly are first compared to the observed eddy fluxes associated with the NAO (Figure 1b,d). The observed transients are defined by the 2-8dy filtered components of the daily reanalysis data, which are then converted to the monthly mean momentum and heat fluxes. After the monthly climatology was removed, the winter-mean anomalies are regressed upon the NAO index, i.e., the PC time series, for 1948-2000. On the other hand, the model represents neither stationary eddies nor low-frequency waves, the transients in the life cycle experiments are simply defined by the deviation from the zonal average, denoted as ( )'. The eddy statistics obtained from the reference integration with $\alpha = 0$ are regarded as 'climatology'; therefore, the time-mean (i.e., 30dy average) anomalies of the eddy flux at each $\alpha$ are obtained by subtracting those at $\alpha = 0$.

The eddy momentum flux anomaly related to the observed NAO has the maximum around the node of the zonal flow dipole, and hence works to reinforce it by the divergence (convergence) of westerly momentum over the easterly (westerly) anomaly region (Figure 1b). The anomalous heat flux is

overall positive, having a broad maximum in 45° -75° N, which indicates that the Atlantic storm track is intensified and shifted to the north for the positive phase of the NAO [e.g., *Hurrell* 1995]. With the choice of $\alpha = +3$, the time-mean anomalous fluxes of momentum and heat, $\left(\overline{u'v'}\right)_a$ and $\left(\overline{v'T'}\right)_a$, capture the observational profiles, except for the narrow meridional scale (Figure 1d).

As shown by the previous studies [*Simmons and Hoskins* 1980; *Thorncroft et al.* 1993; *Akahori and Yoden* 1997; *Balasubramanian and Garner* 1997; *Hartmann and Zuercher* 1998], the eddy life cycle can be morphologically distinctive depending on the polarity of the imposed initial barotropic shear. Namely, for the anticyclonic shear, baroclinic waves tend to break in an ordinary manner, which is called the LC1-type wave breaking, while for the cyclonic shear the waves wrap up away from the jet latitude, called LC2, which persists longer time because the barotropic conversion associated with the wave breaking is greatly suppressed. A similar difference is found between the eddy kinetic energy for positive and negative $\alpha$ (Figure 2a). The baroclinic waves for the initial anticyclonic shear ($\alpha > 0$) grow and decay faster than the reference, while the waves for the cyclonic shear ($\alpha < 0$) grow slowly and do not decay even at the end of integration. The upper-level potential vorticity maps for $\alpha \pm 6$ at day 12 clearly illustrate that they correspond to the LC1 and LC2 cyclones, respectively (Figure 2b,c). It is thus suggested that the barotropic component in $\bar{U}_a$

primarily controls the wave life cycles, but the time-mean heat flux anomaly that is shifted to the north (Figure 1d) is affected by the change in low-level baroclinicity.

In the life cycle experiment that lacks forcing to maintain baroclinically unstable state, the jet's barotropization occurs due to the eddy feedback [*Simmons and Hoskins* 1978]. The initial jet in the reference integration is stabilized by the growth of the baroclinic waves (not shown), as well as shifted poleward in the upper troposphere by the eddy momentum forcing at around days 10-15 (shading in Figure 3). The wave breaking that causes $\overline{u'v'}$ can also occur for both positive and negative $\alpha$, but in a different manner (Fig. 3, right panels). Consistent with the LC1/LC2 paradigm and with observations [*Riviere and Orlanski* 2007; *Martius et al.* 2007], the wave breaks anticyclonically for the anticyclonic shear and vice versa; the former (latter) has more (less) tilted and hence stronger (weaker) $\overline{u'v'}$ compared to that in the reference integration. Consequently, the initial flow dipole is intensified for both polarities, indicating the positive eddy-mean flow feedback (contours in Figure 3).

In order to understand what character in the NAO-like flow dipole is responsible for the positive eddy feedback, we performed two additional sets of experiments: one is similar to the standard set discussed previously (STD) but $\overline{U}_a$ is replaced with its barotropic component, denoted as UBR, and another is the set in which the meridional profile of $\overline{U}_a$ is shifted to south

such as to be symmetric with respect to $\bar{U}_b$ (USY).

The upper-tropospheric zonal-mean wind anomalies at $\alpha = \pm 6$ are compared among the three experiments (Figure 4a,b). For both STD and UBR, the equilibrated zonal wind anomaly (defined by the average during the last 10 days of the integration) is quite similar to $\bar{U}_a$ but with larger magnitude. A careful comparison shows, however, that the intensification of $\bar{U}_a$ is most conspicuous at $\alpha = +6$ in STD, which is also visible in Figure 3a,b, indicating the strongest positive feedback. Interestingly, the equilibrium zonal wind anomalies in USY are similar to those in STD and UBR; they are shifted to north by about 10 degrees from $\bar{U}_a$ given in USY. This suggests that the meridional profile of $\bar{U}_a$ that is asymmetric about the mean jet (Figure 1c) is favored by the eddy feedback.

The degree of the positive eddy feedback is systematically examined by plotting $\partial F_{ya} / \partial \bar{U}_a$, where $F_{ya} \equiv -(\partial_\varphi \overline{u'v'})_a$ is the time-mean anomaly of the eddy momentum forcing to $\bar{U}$ (Fig. 4c). This quantity, called the eddy feedback factor, is calculated by regressing $F_{ya}$ on to $\bar{U}_a$, and measures the growth rate of the initial zonal wind anomaly due to interaction with baroclinic eddies. As inferred from Fig. 4a,b, the feedback factor is always positive in STD but has the maximum with $\alpha = +6$, when the e-folding time is about 10 days. Beyond this shear, the positive eddy feedback is drastically weakened, and is even insignificant at $\alpha \geq +12$. With too strong anticyclonic shear, baroclinic waves break too fast, which is not efficient in reinforcing the

initial zonal wind anomaly (not shown). The above feature suggests that the positive NAO is favored by the eddy feedback, which, however, is limited for moderate amplitude of the NAO.

When the initial shear is purely barotropic, the feedback factor is reduced (enhanced) for positive (negative) $\alpha$ (green curve in Figure 4c). Since the anticyclonic shear in STD accompanies intensified baroclinicity to the mean baroclinic zone, and vice versa, the positive feedback found in STD partly arises from change in the low-level baroclinicity. In the presence of the surface stress that is not included in the life cycle experiments, the eddy feedback observed in UBR will not happen because the boundary layer zonal wind anomaly is readily decelerated and hence accompanies a strong vertical shear aloft. Such a change in $\bar{U}$ will finally result in the eddy feedback close to that obtained in STD.

## 4. Summary and discussion

In the present study, dynamical interaction between baroclinic waves and a meridional dipole of the zonal-mean flow anomaly that is an essence of the observed NAO/NAM is examined by using an idealized dynamical model of the atmosphere. A series of baroclinic eddy life cycle experiments shows that the momentum fluxes due to baroclinic waves, modulated by the initial zonal flow anomaly, tend to reinforce it regardless of the polarity of the imposed NAO-like sheared flow. The degree of this positive feedback,

however, depends on the amplitude and meridional, as well as vertical, structure of the shear. In short, the feedback efficiently works for moderate amplitude of the zonal-flow anomaly with the anticyclonic shear, suggesting that the positive NAO is more preferred by the eddy-mean flow interaction.

Our numerical experiments provide clues for the NAO-eddy interaction, but are still highly idealized, and have a gap with the observations, which show, for example, that the wave breaking associated with the blocking also affects the NAO [*Woolings et al.* 2008; *Strong and Magnusdottir* 2008], and that the regions of LC1/LC2 wave breaking are longitudinally different [*Martius et al.* 2007]. Yet, we believe that the results presented here are the essence of the interaction between the NAO/NAM and synoptic waves, which could be further qualified with a hierarchy of models towards reality.

**Acknowledgments.** MW is grateful to F.-F. Jin for stimulating discussion. This work is partially supported by a Grant-in-Aid for Scientific Research from MEXT, Japan.

## References

Akahori, K., and S. Yoden (1997), Zonal flow vacillation and bimodality of baroclinic eddy life cycles in a simple global circulation model. *J. Atmos. Sci.*, 54, 2349-2361.

Balasubramanian, G., and S. Garner (1997), The role of momentum fluxes in

shaping the life cycle of a baroclinic wave. *J. Atmos. Sci.,* 54, 510-533.

Franzke, C., S. Lee, and S. B. Feldstein (2004), Is the North Atlantic Oscillation a breaking wave? *J. Atmos. Sci.,* 61, 145-160.

Hartmann, D. L., and P. Zuercher (1998), Response of baroclinic life cycles to barotropic shear. *J. Atmos. Sci.,* 55, 297-313.

Hasumi, H., and S. Emori (2004), K-1 coupled model (MIROC) description. K-1 tech. report. Center for Climate System Research, Univ. of Tokyo, 34pp.

Hurrell, J. W. (1995), Decadal trends in the North Atlantic Oscillation region temperatures and precipitation. *Science*, 269, 676-679.

Jin, F.-F., L.-L. Pan, and M. Watanabe (2006a), Dynamics of synoptic eddy and low-frequency flow feedback. Part I: A linear closure. *J.Atmos.Sci.*, 63, 1677-1694.

Jin, F.-F., L.-L. Pan, and M. Watanabe (2006b), Dynamics of synoptic eddy and low-frequency flow feedback. Part II: A theory for low-frequency modes. *J.Atmos.Sci.*, 63, 1695-1708.

Kistler, R., and Co-authors (2001), The NCEP-NCAR 50-year reanalysis: Monthly means CD-ROM and documentation. *Bull. Amer. Meteor. Soc.*, 82, 247-267.

Kug, J. S., and F.-F. Jin (2009), Left-hand rule for synoptic eddy feedback on low-frequency flow. *Geophys. Res. Lett.*, in press.

Lau, N.-C. (1988), Variability of the observed midlatitude storm tracks in relation to low-frequency changes in the circulation pattern. *J. Atmos.*

*Sci.,* 45, 2718-2743.

Lorenz, D. J., and D. L. Hartmann (2003), Eddy-zonal flow feedback in the Northern Hemisphere winter. *J. Climate*, 16, 1212-1227.

Martius, O., C. Schwierz, and H. Davies (2007), Breaking waves at the tropopause in the wintertime Northern Hemisphere: Climatological analyses of the orientation and the theoretical LC1/2 classification. *J. Atmos. Sci.,* 64, 2576-2592.

Orlanski, I. (2003), Bifurcation in eddy life cycles: Implications for storm track variability. *J. Atmos. Sci.,* 60, 993-1023.

Rivière, G., and I. Orlanski (2007), Characteristics of the Atlantic storm-track eddy activity and its relation with the North Atlantic Oscillation. *J. Atmos. Sci.,* 64, 241-266.

Simmons, A. J., and B. J. Hoskins (1978), The life cycles of some non-linear baroclinic waves. *J. Atmos. Sci.,* 35**,** 414-432.

Simmons, A. J., and B. J. Hoskins (1980), Barotropic influences on the growth and decay of nonlinear baroclinic waves. *J. Atmos. Sci.*, 37, 1679-1684.

Strong, C., and G. Magnusdottir (2008), Tropospheric Rossby wave breaking and the NAO/NAM. *J. Atmos. Sci.,* 65, 2861-2876.

Thorncroft, C. D., B. J. Hoskins, and M. McIntyre (1993), Two paradigms of baroclinic-wave life-cycle behavior. *Quart.J.R.Met.Soc.,* 119, 17-55.

Vallis, G. K., E. P. Gerber, P. J. Kushner, and B. A. Cash (2004), A

mechanism and simple dynamical model of the North Atlantic Oscillation and annular modes. *J. Atmos. Sci.,* 61, 264-280.

Watanabe, M., and M. Kimoto (2000), Atmosphere-ocean thermal coupling in the North Atlantic: A positive feedback. *Quart.J.R.Met.Soc.*, 126, 3343-3369; Corrigendum. *Quart.J.R.Met.Soc.*, 127, 733-734.

Watanabe, M., and F.-F. Jin (2004), Dynamical prototype of the Arctic Oscillation as revealed by a neutral singular vector. *J.Climate*, 17, 2119-2138.

Wittman, M., A. Charlton, and L. Polvani (2007), The effect of lower stratospheric shear on baroclinic instability. *J. Atmos. Sci.*, 64, 479-496.

Woolings, T., B. J. Hoskins, M. Blackburn, and P. Berrisford (2008), A new Rossby wave-breaking interpretation of the North Atlantic Oscillation. *J. Atmos. Sci.*, 65, 609-626.

## Figure Captions

**Figure 1:** (a) Observed zonal wind anomaly associated with the NAO (color contours; the interval is 1 $ms^{-1}$), imposed on the winter climatological wind (shading) and potential temperature (thin contours; a thick contour denotes 330 K isoline) averaged over the North Atlantic sector. (b) Vertically averaged meridional momentum and heat flux anomalies associated with the NAO. (c)-(d) As in (a)-(b), but for the idealized fields used in the life cycle experiments. The model anomalies are obtained at α=+3.0.

**Figure 2:** (a) Time evolution of the eddy kinetic energy at different α. The red (blue) curves represent the life cycles with anticyclonic (cyclonic) shear. (b)-(c) Potential vorticity maps on 330 K isentrope at day 12 at $\alpha = \pm 6$.

**Figure 3:** (a) Time evolution of the zonal-mean zonal wind anomaly (contour; the interval is 5 $ms^{-1}$) at α=+6. The gray shading denotes the evolution of the zonal wind in the reference experiment. The right panel shows evolution of the 1PVU contours on the 330K isentrope during days 9-14. (b) As in (a), but for α=-6. The PV contours are presented during days 11-16.

**Figure 4:** Initial and equilibrated (thin and thick curves) zonal wind at σ=0.29; (a) α=+6 and (b) α=-6. The red, blue, and green curves represent the results obtained from STD, UBR, and USY experiments. (c) Eddy feedback factors at σ=0.29 as a function of α. The open symbols indicate the significant correlation at the 95% level between $\overline{U}_a$ and $F_{ya}$.

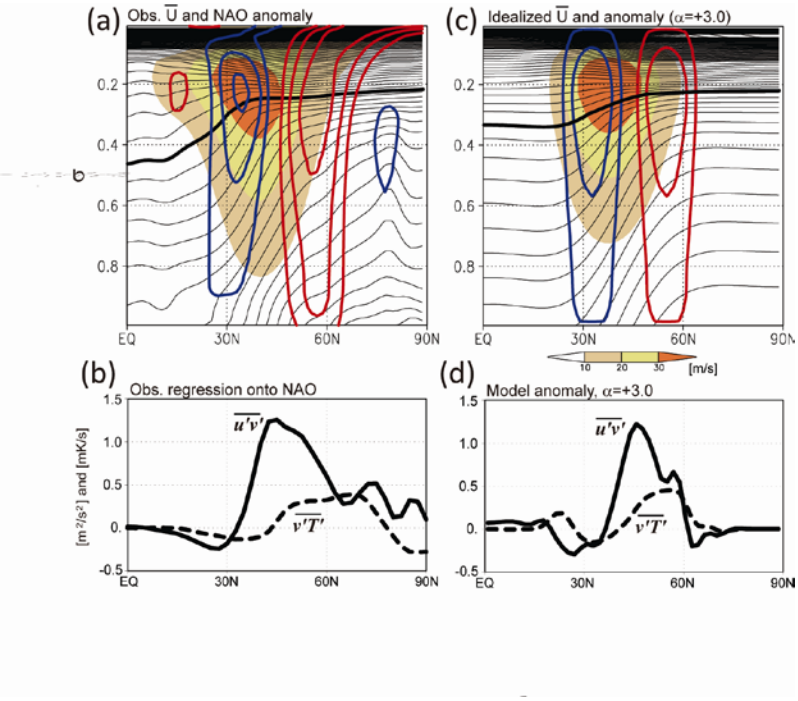
(a) Obs. $\overline{U}$ and NAO anomaly
(c) Idealized $\overline{U}$ and anomaly (α=+3.0)
σ
0.2
0.4
0.6
0.8
EQ
30N
60N
90N
10
20
30
[m/s]
(b) Obs. regression onto NAO
(d) Model anomaly, α=+3.0
$\overline{u'v'}$
$\overline{v'T'}$
[m²/s²] and [mK/s]
1.5
1.0
0.5
0.
-0.5

Figure 1

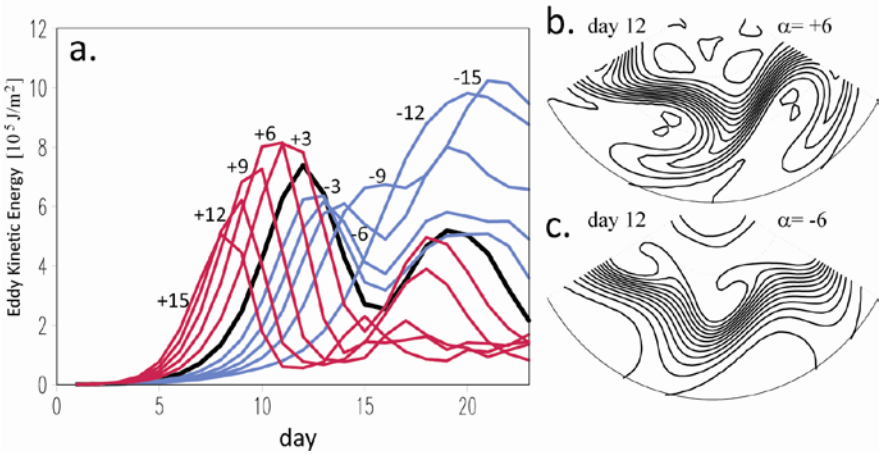
a.
b. day 12
α= +6
c. day 12
α= -6
Eddy Kinetic Energy [10^5 J/m^2]
day
+15
+12
+9
+6
+3
-3
-6
-9
-12
-15

Figure 2

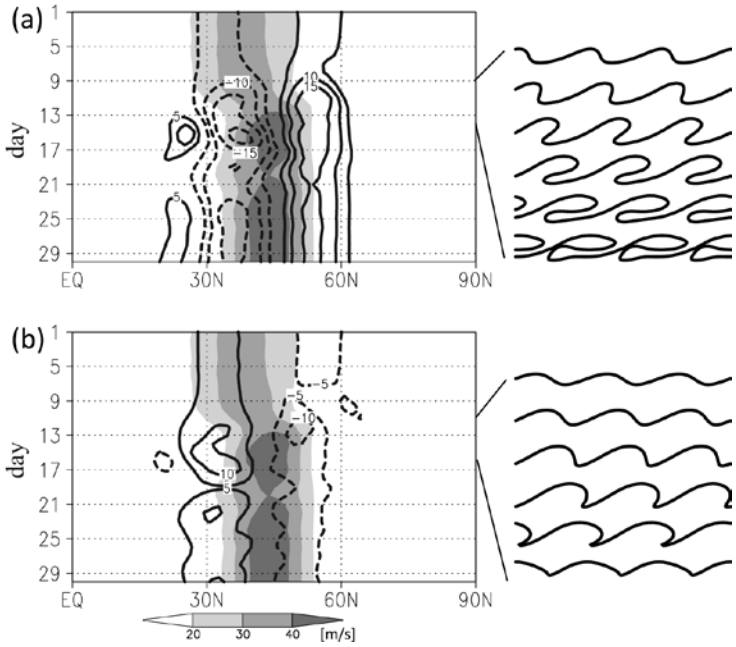


Figure 3

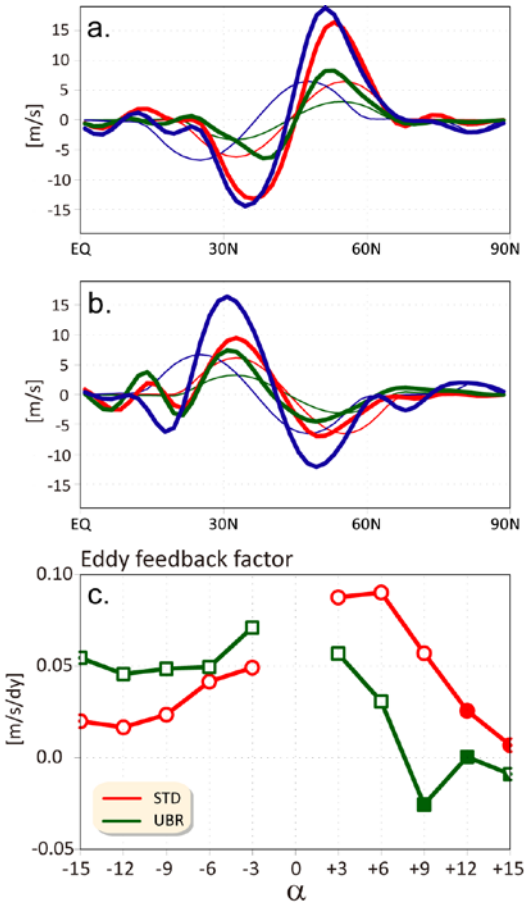
a.
[m/s]
15
10
5
0
-5
-10
-15
EQ
30N
60N
90N
b.
[m/s]
15
10
5
0
-5
-10
-15
EQ
30N
60N
90N
Eddy feedback factor
c.
[m/s/dy]
0.10
0.05
0.0
-0.05
STD
UBR
-15
-12
-9
-6
-3
0
+3
+6
+9
+12
+15
α

Figure 4